Eur. Phys. J. B **36**, 175–181 (2003)
DOI: 10.1140/epjb/e2003-00332-y

THE EUROPEAN PHYSICAL JOURNAL B

Suppression of incommensurate spin-density waves in thin epitaxial Cr(110) layers of a V/Cr multilayer

H. Fritzsche[1,a], S. Bonn[2], J. Hauschild[2], K. Prokes[2], and J. Klenke[2]

[1] National Research Council Canada, Chalk River Laboratories, Chalk River, ON, K0J 1J0, Canada
[2] Hahn-Meitner-Institut, Glienicker Strasse 100, 14109 Berlin, Germany

Received 17 June 2003 / Received in final form 28 August 2003
Published online 8 December 2003 –

Abstract. We observed a complete suppression of the incommensurate spin-density wave in thin Cr layers of a V/Cr multilayer in a temperature range from 550 K down to 2 K. The (110)-oriented V/Cr multilayer consisting of 30 nm thick Cr layers and 5 nm thick V layers was investigated by neutron and X-ray diffraction (XRD). From the XRD experiments we were able to determine that the epitaxial strain of the Cr layers in the V/Cr multilayer is about 90% larger than in earlier studied Fe/Cr(110) multilayers. That leads to a completely different magnetic phase diagram as revealed by neutron diffraction experiments. The existence of the commensurate antiferromagnetic structure in the Cr layers can be observed in the whole temperature range without a phase transition to an incommensurate spin-density wave at lower temperatures. In order to elucidate the proximity effects further we also performed experiments in an external magnetic field. Up to a field of 4 T we found no change in the magnetic structure of the Cr films whereas in earlier experiments on Fe/Cr(110) multilayers we could observe a strong perpendicular pinning of the Cr polarization to the Fe magnetization.

PACS. 75.30.Fv spin-density waves – 75.70.-i magnetic properties of thin films, surfaces, and interfaces – 61.12.-q Neutron diffraction and scattering

1 Introduction

The discovery of an antiferromagnetic structure in Cr samples by Shull and Wilkinson [1] in 1953 initiated a huge amount of scientific investigations on all physical properties of chromium. Neutron diffraction experiments always played a key role in revealing the details of the magnetic structure of chromium. In the beginning the influence of the sample preparation on the magnetic properties of Cr bulk samples were the focus of interest. Shull et al. [1] used a polycrystalline sample and found a commensurate antiferromagnetic structure (AF_0) with a Néel temperature T_N of about 450 K. This commensurate structure is characterized by an antiparallel alignment of the Cr polarization vectors of corner atoms and body-centered atoms within the bcc unit cell. In 1959, Corliss et al. [2] working on a Cr single crystal found for the first time the incommensurate spin-density wave (ISDW). This ISDW corresponds to a sinusoidal modulation of the antiferromagnetic arrangement of the Cr moments and in neutron diffractometry it shows up as satellites around the Cr{100} positions. The modulation period is temperature dependent and changes from 6 nm at 2 K to 8 nm at 310 K.

After the detailed neutron diffraction study of Bacon [3] the magnetic phase diagram of Cr single crystals was clarified. Cr orders at $T_N = 311$ K as an antiferromagnet with a transverse ISDW, the so-called AF_1 structure, i.e. with the Cr polarization vector perpendicular to the direction of the modulation period. At a temperature of 123 K an additional phase transition occurs from the transversal ISDW to the longitudinal ISDW (AF_2 structure) with the polarization vectors parallel (or antiparallel) to the direction of the modulation period.

The deviation in Cr polycrystalline samples from the above described ideal behavior could be explained by strain-induced effects [4–6]. The most significant features in these strained Cr samples were the elevation of T_N from 311 K to about 450 K and the coexistence over a wide temperature range of the commensurate AF_0 structure and the incommensurate AF_1 and AF_2 structure. Consequently, the phase transitions from AF_0 to AF_1 and from AF_1 to AF_2 are not sharply defined but are smeared over a large temperature range [4–6].

The observation of an oscillating exchange coupling of ferromagnetic films across nonmagnetic spacer layers in Fe/Cr multilayers [7] lead to a renaissance of the investigation of the magnetic structure of Cr. In addition to the traditional neutron diffraction technique the nuclear methods

[a] e-mail: helmut.fritzsche@nrc.gc.ca

of perturbed angular correlation (PAC) spectroscopy [8] as well as ^{119}Sn Mössbauer spectroscopy [9,10] was used to reveal the magnetic structure of thin Cr films.

Most of the experiments were performed either on (100)-oriented single Cr films or on (100)-oriented Fe/Cr multilayers. For Cr films with a thickness $t_{\mathrm{Cr}} > 5$ nm the phase diagram strongly depends on temperature. Generally, there is a phase transition from the AF_0 structure to the paramagnetic phase at temperatures far above the bulk Néel temperature [11–14]. When lowering the temperature a phase transition to an ISDW is observed. For films with $t_{\mathrm{Cr}} < 5$ nm either the AF_0 phase [11] or the paramagnetic phase was observed [8,15]. Investigations on (110)-oriented Fe/Cr multilayers [16–18] with $t_{\mathrm{Cr}} = 30$ nm showed a similar temperature dependence as the (100)-oriented Cr films.

In order to study the influence of the ferromagnetic layer on the magnetic structure of the Cr layers it is important to perform experiments with Cr layers in contact with paramagnetic layers. In literature experiments are reported on V/Cr multilayers [10], Ag/Cr multilayers [19], Sn/Cr multilayers [20] or on Cu or Pd covered Cr single films [21]. We chose V as paramagnetic material for our investigations and present a detailed neutron diffraction study on a V/Cr(110) multilayer with $t_{\mathrm{Cr}} = 30$ nm. We also applied an external magnetic field in order to compare directly to earlier investigations on Fe/Cr(110) multilayers [17] which revealed a perpendicular pinning of the Cr polarization to the Fe magnetization. Additional information on the strain in the Cr layers could be obtained by performing X-ray diffraction (XRD) experiments.

2 Experimental details

The multilayer was prepared in ultrahigh vacuum by means of molecular beam epitaxy on $Al_2O_3(11\bar{2}0)$ single crystals, covered with a buffer layer of 100 nm V(110). The deposition rates were 0.013 nm/s for the V(110) buffer, 0.014 nm/s for the Cr(110) layers, and 0.01 nm/s for the V(110) spacing layers, respectively. The preparation temperature was 520 K in order to get a sample of good crystalline quality and smooth interfaces as was checked with standard techniques of surface science like low energy electron diffraction and Auger electron spectroscopy. The thickness of the Cr layers was $t_{\mathrm{Cr}} = 30$ nm and the thickness of the V layer $t_{\mathrm{V}} = 5$ nm. The V/Cr bilayer was repeated 13 times in order to get a reasonable signal-to-noise ratio for the neutron diffraction experiments.

The antiferromagnetic structure of the Cr layers has been investigated by neutron diffraction on the triple-axis spectrometer E1 and the two-axis diffractometer E4 at the Hahn-Meitner-Institut, Berlin. We used a pyrolytic graphite monochromator to select a wavelength of $\lambda = 0.24$ nm together with a graphite filter that reduces the $\lambda/2$ contribution of the monochromator by a factor of about 5000. We applied an external vertical magnetic field using the VM3 magnet of the Hahn-Meitner-Institut.

As a quantitative measure for the intensity of the Bragg reflection we took the integrated intensity around the corresponding reflection. Due to the shape of the sample the intensity is strongly influenced by geometrical effects which depend on the sample orientation with respect to the neutron beam and detector. Therefore, we normalized the intensity of the magnetic Cr{100} reflections measured with λ to the intensity of the structural Cr{200} reflections measured with $\lambda/2$=0.12 nm by removing the $\lambda/2$ filter. This has the additional advantage that eventual beam inhomogeneities are also eliminated.

The X-ray measurements were performed on a two-axis diffractometer (model D8 ADVANCE, Bruker-axs) using Cu $K\alpha$ radiation. The instrument was equipped with a pyrolytic graphite monochromator in front of the detector. The epitaxial strain of the Cr layers was calculated from the Cr Bragg peak positions as determined from θ-2θ scans. If the crystalline quality is very high the Cu $K\alpha_1$ radiation [22] with $\lambda = 0.1540593$ nm and the Cu $K\alpha_2$ radiation [22] with $\lambda = 0.1544414$ nm can be resolved. In cases when the double peak could not be resolved we took the relative intensity $I(K\alpha_2)/I(K\alpha_1) = 0.52$ to calculate the weighted mean of Cu $K\alpha_1$ and Cu $K\alpha_2$ resulting in $\lambda = 0.15419$ nm for the Cu $K\alpha$ radiation [22].

3 X-ray diffraction

The structural properties of the multilayer was checked by X-ray diffraction (XRD). In order to determine the out-of-plane lattice constant of the Cr layers we performed θ-2θ scans. For high precision measurements it is very important to calibrate the instrument with a well-known standard sample. We took the $Al_2O_3(11\bar{2}0)$ substrate reflections to calibrate the 2θ-axis. With the lattice constant [23] $a = 0.4759$ nm we can calculate the out-of-plane lattice spacing $d = a/2$ and the corresponding 2θ-value as given in Table 1. The θ-2θ-scan of the $Al_2O_3(11\bar{2}0)$ reflection with the calibrated θ-axis is shown in Figure 1a. For the substrate reflection the doublet of the Cu $K\alpha$ radiation is clearly observable. Therefore, the calibration could be done with high accuracy.

The Cu $K\alpha$ doublet could not be resolved for the V(110) and Cr(110) reflection of the multilayer as can be seen from Figure 1b. Therefore, we took the averaged λ of the Cu K_α radiation to calculate the Cr out-of-plane lattice spacing $d = (0.2033 \pm 0.0001)$ nm. That corresponds to an out-of-plane strain $\epsilon_o = (-0.0030 \pm 0.0007)$ along [110] compared to the bulk value [24] of 0.20393 nm. An overview is given in Table 1.

This measured out-of-plane compression can be interpreted as a Poisson contraction due to the in-plane stress. The in-plane strain ϵ_i can be easily estimated under the assumption that the in-plane stress is homogeneous. Then the minimization of the elastic energy leads to the expression [25]

$$\epsilon_i = -\epsilon_o \frac{c_{11} + c_{12} + 2c_{44}}{c_{11} + 3c_{12} - 2c_{44}} \quad (1)$$

with the elastic constants c_{11}, c_{12}, and c_{44}. The Cr bulk values are [26] $c_{11} = 34.8 \times 10^{10}$ Pa, $c_{12} = 6.7 \times 10^{10}$ Pa,

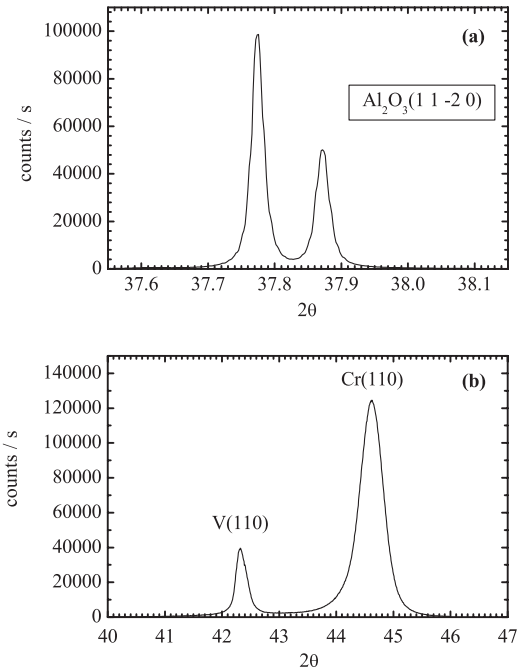

Fig. 1. X-ray θ-2θ diffraction scans a) for the substrate reflection $Al_2O_3(11\overline{2}0)$ and b) the V(110) and Cr(110) reflections. Please note the different scales in a) and b).

Table 1. Measured ($2\theta_{\mathrm{meas}}$) and calculated ($2\theta_{\mathrm{bulk}}$) 2θ values [24,23] for the Cr film and the sapphire substrate. From $2\theta_{\mathrm{meas}}$ the corresponding lattice spacing d was calculated.

	λ (nm)	$2\theta_{\mathrm{meas}}$ (°)	$2\theta_{\mathrm{bulk}}$ (°)	d (nm)
Cr	0.15419	44.568	44.426	0.2033
Al_2O_3	0.15406		37.776	
Al_2O_3	0.15444		37.874	

and $c_{44} = 10.0 \times 10^{10}$ Pa. Inserting these values into equation (1) we get $\epsilon_i = 0.0053 \pm 0.0013$ for the strain along the in-plane directions [001] and $[1\overline{1}0]$.

It is important to note that the calculated lattice constant along with the calculated strain are values which result from an averaging over the whole film. Theoretical calculations [27] and experiments [28] show that the strain relaxation is proportional to the inverse film thickness above the pseudomorphic regime. As a consequence, a large distribution of lattice constants exists. This broad distribution of lattice spacings causes a broad peak in a $\theta - 2\theta$ scan at the Cr(110) position as can be seen in Figure 1b. The evaluation of rocking scans around the Cr(220) reflection gives a grain size of 7.5 nm.

4 Neutron diffraction

The antiferromagnetic structure of Cr was investigated by classical neutron diffraction. The scattering cross section of an unpolarized neutron beam with a magnetization wave $\boldsymbol{M}(\boldsymbol{r})$ can be written as:

$$\frac{d\sigma}{d\Omega} = |\boldsymbol{M}_q|^2 \sin^2 \theta_q \tag{2}$$

where θ_q is the angle between $\boldsymbol{M}$ and $\boldsymbol{q}$ and $\boldsymbol{M}_q$ is the Fourier component of $\boldsymbol{M}(\boldsymbol{r})$. For neutrons generally the contribution of the magnetic and nuclear part to the scattering cross section are of the same order of magnitude. For the case of a bcc crystal it is well-known that the structure factor vanishes for those (HKL) reflections for which the sum $(H + K + L)$ is odd. Hence, the measured intensity at the position of these reflections, e.g. the Cr{100} reflections, is of pure magnetic origin. It is worthwhile to mention that this selection rule is also strictly valid for our Cr film which has a body-centered tetragonal structure because of the strain.

4.1 Temperature dependence of the antiferromagnetic structure

At 295 K we investigated all three independent Cr{100} reflections and scanned along the H, K, and L directions of reciprocal space. The results are shown in Figure 2 for the Cr(001) reflection, in Figure 3 for the Cr(010) reflection, and in Figure 4 for the Cr(100) reflection. These scans are a direct proof of the existence of the commensurate AF_0 structure in the Cr layers. An ISDW would show up in the scans as satellite peaks at about ± 0.04 for transverse scans and at 0.96 and 1.04 for longitudinal scans. That is definitely not visible.

First of all, it is remarkable that we do not observe the same intensity for all three independent Cr{001} reflections because in bulk Cr the probability for all these reflections is a priori the same. According to equation (2) only magnetization components perpendicular to $\boldsymbol{q}$ are contributing to the integrated intensity. Therefore, it is straightforward to calculate the orientation of the polarization $\boldsymbol{S}$. Based on the normalized integrated intensities of the magnetic {001} reflections, shown in Table 2, we obtain for the polarization vector $\left(|S_x|^2, |S_y|^2, |S_z|^2\right) = (0.9, 1.0, 0.2)$ with an error of ± 0.1. This means that the averaged polarization vector is roughly parallel to [221], 19° off the surface normal [110].

We even observed the AF_0 structure down to 2 K without an indication of a phase transition to an ISDW. As can be estimated from Figure 5, a phase transition from the commensurate phase to the paramagnetic state occurs at $T_N \approx 600$ K. The solid line was plotted as a guide to the eye.

4.2 Magnetic field dependence of the antiferromagnetic structure

There are two main results of the investigations on the magnetic field dependence of the antiferromagnetic structure of bulk Cr samples. Firstly, by applying a magnetic field of about 3 T during the sample cooling through

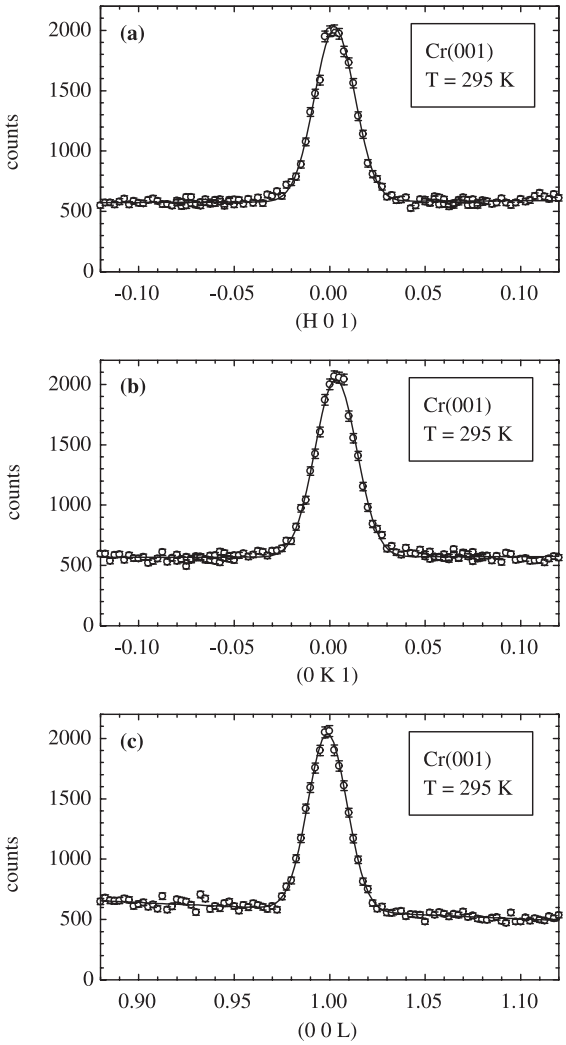

Fig. 2. Neutron diffraction scans in the a) H-direction, b) K-direction, and c) L-direction through the Cr(001) reflection of the V/Cr(110) multilayer, measured at 295 K on E1. The solid line represents a Gaussian fit to the experimental data. All scans shown in Figures 2–4 were measured with the same number of monitor counts.

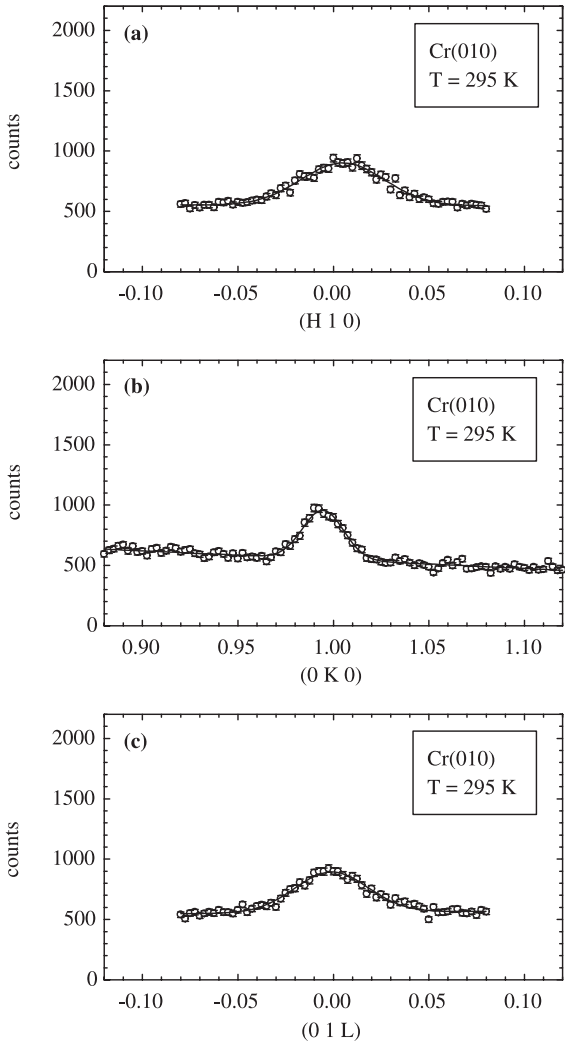

Fig. 3. Neutron diffraction scans in the a) H-direction, b) K-direction, and c) L-direction through the Cr(010) reflection of the V/Cr(110) multilayer, measured at 295 K on E1. The solid line represents a Gaussian fit to the experimental data. All scans shown in Figures 2–4 were measured with the same number of monitor counts.

its Néel temperature (the so-called field-cooling) a single $\boldsymbol{q}$ state can be produced with $\boldsymbol{q}$ being parallel to the magnetic field direction [29]. Secondly, when applying a magnetic field in the transverse SDW state the polarization vector of the domains rotate into a direction perpendicular to the field [30]. Generally, the perpendicular orientation of the polarization of the antiferromagnet is preferred because the perpendicular susceptibility is larger than the one parallel to the field.

Recently, the dependence of the antiferromagnetic structure on magnetic fields in (110)-oriented Fe/Cr multilayers has been reported [17]. The (110) surface creates a uniaxial anisotropy with [001] as the easy axis and $[1\bar{1}0]$ as the hard axis of the Fe magnetization. At 300 K the stable phase is the CSDW with the Cr polarization aligned perpendicular to [001]. When rotating the Fe magnetization from the easy axis into the in-plane hard-axis direction by applying a magnetic field of 0.45 T the intensity of the Cr(001) reflection decreases by a factor of two. That was interpreted as a simultaneous rotation of the Fe and Cr moments pinned together in its initial perpendicular orientation.

In order to study the proximity effects we performed experiments in external fields on V/Cr multilayers as well. That enables us to compare directly the case of nonmagnetic layers to the case of ferromagnetic layers in contact with the Cr layers. As in our previous experiments on the Fe/Cr multilayers we applied the external magnetic field along the in-plane $[1\bar{1}0]$ direction and measured the intensity of the Cr(001) reflection at room temperature as a function of the magnetic field. In Figure 6 the rocking scans around the Cr(001) reflection for a) $\mu_0 H = 0$ T and b) $\mu_0 H = 4$ T are displayed. The rocking curve in a) was measured with 1.2 million monitor counts, whereas the

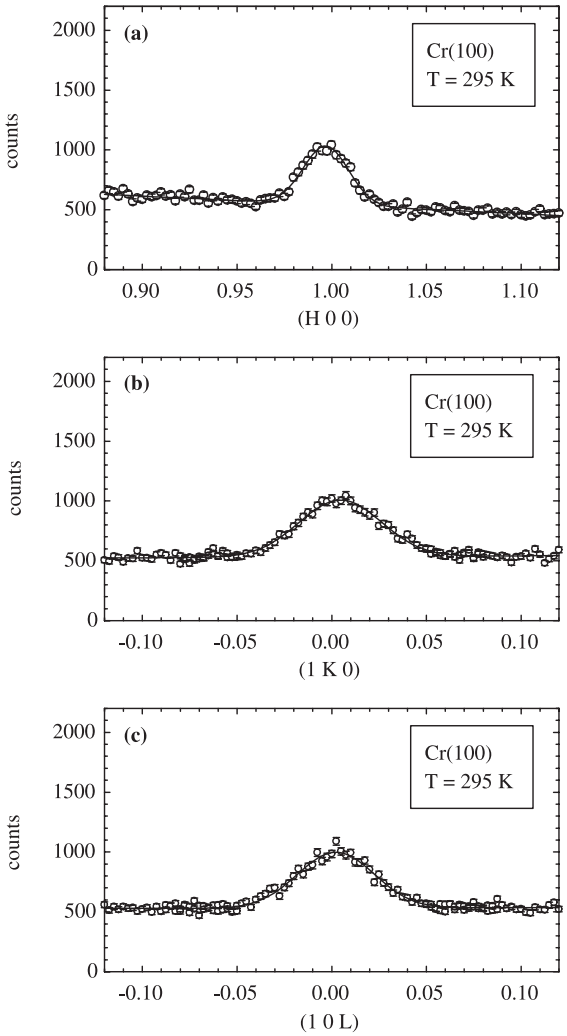

Fig. 4. Neutron diffraction scans in the a) H-direction, b) K-direction, and c) L-direction through the Cr(100) reflection of the V/Cr(110) multilayer, measured at 295 K on E1. The solid line represents a Gaussian fit to the experimental data. All scans shown in Figures 2–4 were measured with the same number of monitor counts.

Table 2. Integrated intensity of the magnetic Cr{001} reflections normalized to the respective nuclear Cr{002} reflections.

Direction	Cr(001)	Cr(010)	Cr(100)
H	1.67 ± 0.04	1.00 ± 0.06	1.08 ± 0.05
K	1.72 ± 0.04	1.16 ± 0.07	1.09 ± 0.05
L	1.69 ± 0.04	0.93 ± 0.06	1.07 ± 0.05

curve displayed in b) was measured for 2 million monitor counts. In order to compare both curves directly, all measured points in a) were multiplied by a factor of 5/3.

From the Gaussian fits displayed in Figure 6 as solid lines we could determine the integrated intensities. For the case of zero field we get $I_0 = 523 \pm 14$ and for the applied field of 4 T we get $I_4 = 871 \pm 16$. After the correction for the monitor counts, i.e. multiplying I_0 by the factor 5/3,

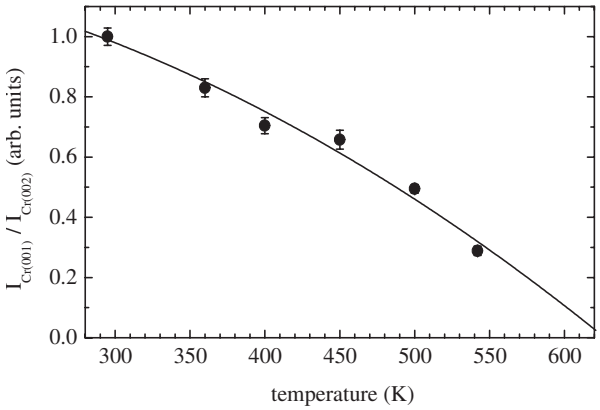

Fig. 5. Temperature dependence of the integrated intensity of the Cr(001) reflection normalized to the integrated intensity of the Cr(002) reflection. The solid line represents a guide to the eye.

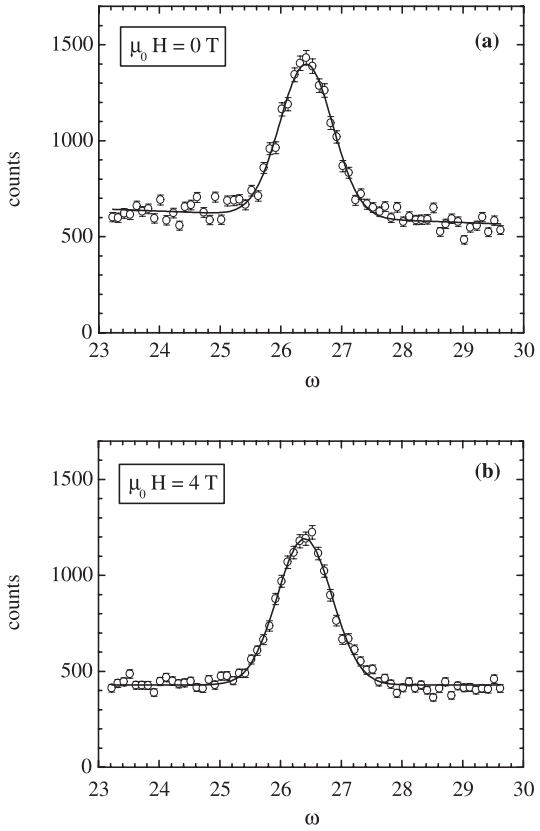

Fig. 6. Rocking scan around the Cr(001) reflection at an external magnetic field of a) 0 T and b) 4 T. The rocking curve in zero field was measured for 1.2 million monitor counts and the curve in a field of 4 T was measured for 2 million monitor counts. In order to compare the graphs directly all measured points in a) were multiplied by a factor of 5/3. The solid lines are Gaussian fits.

the integrated intensity in zero field equals 872 and is the same within the error limits as in a field of 4 T. So, even a magnetic field of 4 T cannot influence the antiferromagnetic structure of these thin Cr layers.

5 Discussion

The neutron diffraction experiments on (110)-oriented V/Cr multilayers reported in this article enables us to compare directly to earlier experiments on Fe/Cr multilayers and to study the proximity effects on the antiferromagnetic structure of thin Cr layers in contact with nonmagnetic and ferromagnetic layers, respectively. The commensurate phase which is stable at room temperature is not due to the presence of a ferromagnetic layer because it exists in the Fe/Cr as well as in the V/Cr multilayer. The enhanced Néel temperature of about 600 K was also observed in both types of multilayers. However, there is a big difference in the temperature dependence of the antiferromagnetic structure for temperatures below room temperature. For the Fe/Cr(110) multilayer a transition to the ISDW is observed whereas for the V/Cr sample only the commensurate phase is observed down to $T = 2$ K. Mössbauer measurements performed on V/Cr multilayers [10] confirm that there is no phase transition below room temperature because the spectra for a Cr film thickness of 8 nm show no difference at room temperature and at 15 K.

When comparing the properties of Fe/Cr and V/Cr multilayers not only the interfaces are electronically different but also the structure of the Cr layers is different because of the different epitaxial strain due to the different lattice constants. For the Fe/Cr system there is only a very small misfit

$$\eta_{\mathrm{Fe/Cr}} = \frac{a_{\mathrm{Fe}} - a_{\mathrm{Cr}}}{a_{\mathrm{Cr}}} = -0.0062 \qquad (3)$$

with the Fe lattice constant [24] $a_{\mathrm{Fe}} = 0.2866$ nm and the Cr lattice constant [24] $a_{\mathrm{Cr}} = 0.2884$ nm. The real epitaxial strain in the Cr layers depends also on the used substrate because the substrate induces strain as well. Obviously, the strain in Fe/Cr multilayers is about the same as in strained bulk Cr crystals because they have similar temperature dependent phase diagrams. For the case of strained Cr bulk samples it was already concluded that the strain is the origin of the commensurate AF_0 structure [4–6] and the coexistence of the ISDW and the CSDW. For Ag/Cr multilayers which exhibit an even smaller misfit of $\eta_{\mathrm{Ag/Cr}} = -0.0028$ only the longitudinal ISDW was observed [19].

However, for the V/Cr multilayer there is a large misfit of $\eta_{\mathrm{V/Cr}} = 0.047$ resulting in an averaged out-of-plane strain of $\epsilon_o = -0.0030$ as measured by XRD and an averaged in-plane strain of $\epsilon_i = 0.0053$ as deduced from elasticity theory. The amount of stress is higher compared to the Fe/Cr multilayers which were prepared on a V(110) single crystal [17,18]. From X-ray measurements we determined $\epsilon_o = (-0.0016 \pm 0.0005)$ and calculated $\epsilon_i = 0.0028 \pm 0.0008$ for these Cr layers. Obviously, the larger amount of strain present in the V/Cr multilayer leads to a complete suppression of a transition to an ISDW at lower temperatures. It is unclear whether the small grain size of 7.5 nm also affects the magnetic properties. In general the magnetic properties depend on the film thickness, e.g. for Fe/Cr multilayers the ISDW is not observable below 5 nm [8,11,15] and measurements on V/Cr multilayers as a function of Cr film thickness [10] show that the Cr magnetism breaks down for film thicknesses below 1 nm. Because of the fact that the grain size is larger than the periodicity of the ISDW we believe that the influence of the grain size is rather limited.

The experiments performed in external magnetic fields showed that the antiferromagnetic structure in the Cr layers remained unchanged up to a field of 4 T. That behaviour is different compared to Cr bulk samples where a magnetic field of about 2 T leads to a reorientation of the Cr polarization perpendicular to the field [30] for those domains with an initial parallel polarization.

6 Conclusion

The performed X-ray and neutron diffraction experiments on V/Cr multilayers and comparison to earlier experiments on Fe/Cr multilayers [17,18] clearly show that strain plays a crucial role for the phase diagram of thin Cr layers. As determined by XRD the strain in the V/Cr(110) multilayer is 90% higher compared to the Fe/Cr(110) multilayer. That higher amount of strain in the V/Cr multilayer suppresses the incommensurate phases in the whole temperature range under investigation, i.e. from 2 K to 550 K in contrast to the Fe/Cr multilayers where a phase transition takes place from the AF_0 structure to the ISDW. In the Ag/Cr system where the misfit is even smaller than in the Fe/Cr multilayers the commensurate phase was not observed [19].

The experiments in external magnetic fields show that the antiferromagnetic structure does not change up to a magnetic field of 4 T. That behavior is different for Cr bulk samples. Furthermore, the comparison with experiments on Fe/Cr(110) multilayers where the Cr polarization could be rotated easily by rotating the Fe magnetization [17] confirms the extraordinary strong exchange coupling at the Fe/Cr interface.

References

1. C.G. Shull, M.K. Wilkinson, Rev. Mod. Phys. **25**, 100 (1953)
2. L.M. Corliss, J.M. Hastings, R.J. Weiss, Phys. Rev. Lett. **3**, 211 (1959)
3. G.E. Bacon, Acta Cryst. **14**, 823 (1961)
4. G.E. Bacon, N. Cowlam, J. Phys. C: Solid State Phys. **2**, 238 (1969)
5. I.S. Williams, E.S.R. Gopal, R. Street, J. Phys. F: Metal Phys. **9**, 431 (1979)
6. I.S. Williams, R. Street, Phil. Mag. B **43**, 893 (1981)
7. P. Grünberg, R. Schreiber, Y. Pang, M.B. Brodsky, H. Sowers, Phys. Rev. Lett. **57**, 2442 (1986)
8. J. Meersschaut, J. Dekoster, R. Schad, P. Belien, M. Rots, Phys. Rev. Lett. **75**, 1638 (1995)
9. K. Mibu, M. Almokhtar, S. Tanaka, A. Nakanishi, T. Kobayashi, T. Shinjo, Phys. Rev. Lett. **84**, 2243 (2000)

10. M. Almokhtar, K. Mibu, A. Nakanishi, T. Kobayashi, T. Shinjo, J. Phys.: Condens. Matter **12**, 9247 (2000)
11. A. Schreyer, C.F. Majkrzak, T. Zeidler, T. Schmitte, P. Bödeker, K. Theis-Bröhl, A. Abromeit, J.A. Dura, T. Watanabe, Phys. Rev. Lett. **79**, 4914 (1997)
12. P. Sonntag, P. Bödeker, A. Schreyer, H. Zabel, K. Hamacher, H. Kaiser, J. Magn. Magn. Mater. **183**, 5 (1998)
13. J. Meersschaut, J. Dekoster, S. Demuynck, S. Cottenier, B. Swinnen, M. Rots, Phys. Rev. B **57**, R5575 (1998)
14. E. Kunnen, S. Mangin, V.V. Moshchalkov, Y. Bruynseraede, A. Vantomme, A. Hoser, K. Temst, Thin Solid Films **414**, 262 (2002)
15. E.E. Fullerton, S. Adenwalla, G.P. Felcher, K.T. Riggs, C.H. Sowers, S.D. Bader, J.L. Robertson, Physica B **221**, 370 (1996)
16. H. Fritzsche, J. Hauschild, T. Nawrath, A. Hoser, S. Welzel, H.A. Graf, H. Maletta, Physica B **276-278**, 590 (2000)
17. H. Fritzsche, J. Hauschild, A. Hoser, S. Bonn, J. Klenke, Europhys. Lett. **49**, 507 (2000)
18. H. Fritzsche, S. Bonn, J. Hauschild, J. Klenke, K. Prokes, G.J. McIntyre, Phys. Rev. B **65**, 144408 (2002)
19. S. Demuynck, J. Meersschaut, J. Dekoster, B. Swinnen, R. Moons, A. Vantomme, S. Cottenier, M. Rots, Phys. Rev. Lett. **81**, 2562 (1998)
20. M. Takeda, K. Mibu, T. Shinjo, J. Suzuki, Y. Endoh, Appl. Phys. A **74**, S1554 (2002)
21. P. Bödeker, A. Schreyer, H. Zabel, Phys. Rev. B **59**, 9408 (1999)
22. J. Härtwig, G. Hölzer, J. Wolf, E. Förster, J. Appl. Cryst. **26**, 539 (1993)
23. *Landolt-Börnstein, new series, group III*, Vol. 7b1 (Springer Verlag, Berlin, 1975)
24. *Landolt-Börnstein, new series, group III*, Vol. 14a (Springer Verlag, Berlin, 1988)
25. H. Fritzsche, *Ph.D. thesis* (TU Clausthal, Clausthal, 1995)
26. *Landolt-Börnstein, new series, group III*, Vol. 29a (Springer Verlag, Berlin, 1992)
27. P. Bruno, J.P. Renard, Appl. Phys. A **49**, 499 (1989)
28. H. Fritzsche, J. Kohlhepp, U. Gradmann, Phys. Rev. B **51**, 15933 (1995)
29. A. Arrott, S.A. Werner, H. Kendrick, Phys. Rev. Lett. **14**, 1022 (1965)
30. S.A. Werner, A. Arrott, M. Atoji, J. Appl. Phys. **39**, 671 (1968)